Heliyon 10 (2024) e32969

Contents lists available at ScienceDirect

Heliyon

journal homepage: www.cell.com/heliyon

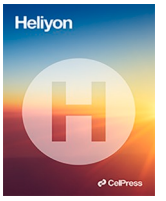

Research article

# Hsa_circRNA_101036 aggravates hypoxic-induced endoplasmic reticulum stress via the miR-21-3p/TMTC1 axis in oral squamous cell carcinoma

Wei Deng [a,1,*], Juan Fu [b,1], Shigeng Lin [a,1], Qitao Wen [a], Liangbin Fu [a], Xiaoze Chen [a]

[a] Department of Oral and Maxillofacial Surgery, Hainan General Hospital (Hainan Affiliated Hospital of Hainan Medical University), Haikou, China
[b] Department of Infectious Diseases, Hainan General Hospital (Hainan Affiliated Hospital of Hainan Medical University), Haikou, China

ARTICLE INFO

*Keywords:*
CircRNA
miR-21-3p
Endoplasmic reticulum stress
Oral squamous cell carcinoma

ABSTRACT

*Objective:* Circular RNAs (circRNAs) have been identified as potential biomarkers and therapeutic targets for various types of cancer, including Oral squamous cell carcinoma (OSCC). Hsa_circRNA_101036 was found to function as a cancer suppressor gene in OSCC; however, the underlying regulatory mechanism remains unclear. We investigated the role of hsa_circRNA_101036 in OSCC development and progression and explored its potential as a therapeutic target.
*Methods:* We performed a bioinformatics analysis and used experimental approaches to investigate the regulatory mechanism of hsa_circRNA_101036. The database StarBase v.2.0 was used to predict potential target-miRNAs of hsa_circRNA_101036. The levels of hsa_circRNA_101036, miR-21-3p, and TMTC2 expression in samples of OSCC cancer tissue (n = 15) and adjacent tissue (n = 15) were determined. We also examined the effects of hsa_circRNA_101036 overexpression on OSCC cell lines by using cell viability, migration, and invasion assays. The proportions of apoptotic cells and the reactive oxygen species (ROS) levels were analyzed by flow cytometry. We also investigated how hsa_circRNA_101036 overexpression affected the levels of miR-21-3p and TMTC2, and endoplasmic reticulum (ER) stress in OSCC cells.
*Results:* The levels of hsa_circRNA_101036 and TMTC2 expression were significantly lower, while miR-21-3p expression was higher in tumor tissues and OSCC cells when compared to adjacent tissues and normal oral fibroblasts, respectively. The levels of HIF-1α and miR-21-3p expression were significantly increased under conditions of hypoxia, while the levels of hsa_circRNA_101036 and TMTC2 were decreased. The expression levels of proteins associated with ER stress, the proportions of apoptotic cells, and the levels of ROS were all increased by hypoxia stimulation. In addition, overexpression of hsa_circRNA_101036, but not mutant hsa_circRNA_101036, was found to enhance the effect of hypoxia on HSC3 and OECM-1 cells. Hsa_circRNA_101036 overexpression suppressed tumor growth and induced ER stress. Finally, knockdown of miR-21-3p had the same effect as overexpression of hsa_circRNA_101036.
*Conclusion:* Our findings suggest that hsa_circRNA_101036 plays a critical role in the development and progression of OSCC. Overexpression of hsa_circRNA_101036 aggravated ER stress, and

* Corresponding author. Department of Oral and Maxillofacial Surgery, Hainan General Hospital (Hainan Affiliated Hospital of Hainan Medical University), 19 Xiuhua Road, Haikou, 570311, China.
*E-mail address:* dengweisums@sina.com (W. Deng).
[1] Authors contributed equally in this work.

https://doi.org/10.1016/j.heliyon.2024.e32969
Received 25 July 2023; Received in revised form 12 June 2024; Accepted 12 June 2024
Available online 13 June 2024

increased cell apoptosis and ROS production in OSCC under hypoxic conditions. Hsa_circRNA_101036 up-regulated TMTC2 expression by sponging miR-21-3p in OSCC.

## 1. Introduction

Oral squamous cell carcinoma (OSCC), which is a severe malignancy with a high rate of metastasis and recurrence, accounts for >90 % of oral cancers [1]. Despite the development of new diagnostic and treatment methods, the 5-year survival rate of OSCC patients does not exceed 50 % [2]. The ability of tumor cells to evade apoptosis makes the situation worse. Therefore, a better understanding of the mechanisms of OSCC cell apoptosis could help to identify some precise targets for treatment of OSCC.

Circular RNAs (circRNAs) comprise a family of endogenous noncoding RNA with a circular structure. They are generated during RNA splicing and arise from exons, introns, or exons-introns [3]. Lacking of the 3′ and 5′ ends, circRNAs have a longer half-life and are more stable than linear RNAs [4]. CircRNAs are widely distributed in multiple human cells and most are conserved [5]. CircRNAs can serve as antagonists by interacting with RNA-binding proteins [6], and thereby regulate gene expression. Moreover, circRNAs can alter gene expression via post-transcriptional regulation by acting as sponges of microRNAs (miRNAs) to inhibit the binding between an miRNA molecule and its target mRNA [7]. Many circRNAs have been found to be abnormally expressed in multiple cancer types [8,9]. Numerous studies have shown that various circRNAs play important roles in cancer progression [10,11], and many circRNAs have been studied for their role in OSCC. For example, circ_0009128 was found to be up-regulated cancer tissues and related to the malignant progression of OSCC. By targeting MMP9, circ_0009128 stimulated OSCC tumor growth and provoked epithelial-mesenchymal transition (EMT) [12]. Hsa_circ_0005379 was found to be abnormally decreased in OSCC tissues, and its overexpression inhibited the tolerance of OSCC to cetuximab [13]. Shi et al. reported that circGDI2 functions as a cancer suppressor gene by sponging miR-454-3p to regulate FOXF2 expression [14]. As an exon circRNA, hsa_circRNA_101036 is produced from splicing of the TMTC1 mRNA precursor. Previously, we reported that hsa_circRNA_101036 inhibited OSCC cell proliferation, invasion, and promoted apoptosis, cytokine release, and endoplasmic reticulum stress [15]. However, its underlying mechanisms in OSCC remain unclear. In the present study, we investigated the role of hsa_circRNA_101036 in OSCC development and progression and explored its potential as a therapeutic target.

A hypoxic microenvironment is a common feature of malignant tumors and contributes to tumor progression, resistance to therapy, and a poor clinical outcome. Hypoxia-inducible factors (HIFs) and their target genes, such as vascular endothelial growth factor (VEGF) and platelet-derived growth factor (PDGF), are correlated with a poor prognosis for OSCC patients [16]. However, the mechanism by which OSCC cells resist hypoxia is not entirely clear. The endoplasmic reticulum (ER) is equipped with a quality control system for protein synthesis. Disulfide bonds and glycosylation formed during the post-translational modification of a protein are dependent on oxygen [17]. Under hypoxic conditions, misfolded proteins accumulate in the ER lumen and trigger an unfolded protein response (UPR). Studies of ER stress in OSCC cells can help to understand its mechanism in resisting hypoxia. Transcriptional reprogramming was induced by three ER stress sensors, which activated transcription factor-6 (ATF6), inositol-requiring enzyme-1α (IRE1α), and protein kinase R-like endoplasmic reticulum kinase (PERK), respectively, consequently affecting the stress response pathways [18]. In solid tumors, cancer cells maintain ER homeostasis to promote cell survival, metastasis, and therapy resistance [19,20]. In addition, ER stress is strongly associated with a hypoxic external environment. HIF-1α can regulate the expression and activity of UPR sensors [21]. Therefore, ER stress under hypoxic conditions plays a vital role in the fate of cancer cells and a patient's prognosis. In this study, we detected changes in hsa_circRNA_101036 expression in OSCC cells under hypoxic conditions. We also performed a bioinformatics analysis to predict the potential target miRNAs of hsa_circRNA_101036. In addition, we examined the effects of hsa_circRNA_101036 overexpression and an miR-21-3p inhibitor on OSCC cell lines by performing cell viability, migration, and invasion assays.

## 2. Materials and methods

### 2.1. Collecting sample

Samples of tumor tissue and paracancerous tissue were obtained from 15 OSCC patients who underwent surgery at Hainan General Hospital. None of the patients had received any prior radiation therapy or chemotherapy. The mean age of the patients was 52.2 ± 3.5 years. There were 4 Phase I (TNM) patients and 11 Phase II patients. All patients provided their written informed for study participation, and the study protocol was approved by the Medical Ethics Committee of Hainan General Hospital (Med-Eth-Re [2023]44).

### 2.2. Cell transfection

Human oral fibroblasts (hOMFs) and 5 OSCC cell lines (SCC-25, HSC3, OECM-1, HN6, and FaDu) were purchased from Procell (Wuhan, China). The cells were cultured in Dulbecco's modified Eagle's medium (DMEM) containing 10 % fetal bovine serum (FBS) at 37 °C in a humidified atmosphere. For normoxia-treated cells, air with 21 % $O_2$ was provided. For hypoxia-treated cells, air with approximately 5 % $O_2$ was provided by a Micro aerobic gas production package (MGC, Tokyo, Japan). To investigate the effect of hsa_circRNA_101036, vectors with its wild or mutant sequence were constructed by GeneScript Biotech Co., Ltd. (Nanjing, China) for overexpression. Empty pCD5-ciR plasmids served as controls. An miRNA inhibitor, negative control, and miR-21-3p inhibitor (5′-

AGACAGCCCATCGACTGGTGTTGCC-3′) were purchased from Ribobio (Guangzhou, China). Finally, HSC3 and OECM-1 cells were transfected with the above materials according to the previous description [22] and using Lipofectamine 3000 (ThermoFisher Scientific, Waltham, MA, USA).

### 2.3. Quantitative polymerase chain reaction

Total RNA was extracted using Trizol reagent (Invitrogen, Waltham, MA, US); after which, a 1 μg sample of total RNA from each group was reverse transcribed into cDNA using a PrimeScript RT Master Mix kit (Takara, Japan). The reverse transcription primer for miR-21-3p was 5-CTCAACTGGTGTCGTGGAGTCGGCAATTCAGTTGAGACAGCCC-3. The quantitative polymerase chain reaction (qPCR) was performed on a StepOnePlusTM Real-Time PCR Instrument (ThermoFisher Scientific) and using ChamQ SYBR qPCR Master Mix (Vazyme, Nanjing, China). The levels of mRNA and miRNA level were normalized to those of GAPDH and U6, respectively. The primer sequences used in this study are listed in Table S1. The PCR reaction conditions were as follows: 94 °C for 2 min; 94 °C for 20 s, 58 °C for 20 s, and 72 °C for 20 s (40 cycles). Finally, relative mRNA expression levels were calculated using the $2^{-\Delta\Delta CT}$ method.

### 2.4. Western blotting

A radioimmunoprecipitation assay lysis buffer containing protease and phosphatase inhibitors (ThermoFisher Scientific) was used to extract the total protein. Next, a 30 μg sample of total protein from each extract was separated by 12 % sodium dodecyl sulfate polyacrylamide gel electrophoresis; after which, the protein bands were transferred onto PVDF membranes (Millipore, Burlington, MA, USA), which were subsequently blocked with 5 % bovine serum albumin [23]. The membranes were then soaked in a solution containing primary antibodies against TMTC2 (PA5-55466, 1:2000; Invitrogen), cleaved caspase 3 (ab32042, 1:500; Abcam, Cambridge, UK), *p*-eIF2α (ab32157, 1:200; Abcam), CHOP (ab11419; Abcam), p-P38 (ab178867, 1:1000; Abcam) or β-actin (ab8226, 1:5000; Abcam) for 1 h at room temperature. Next, the membranes were washed with TBST and then soaked in a solution containing a horseradish peroxidase-conjugated secondary antibody (ab6721, 1:10000; Abcam) for 1 h. The immunostained bands were visualized via enhanced chemiluminescence (ThermoFisher Scientific).

### 2.5. Dual-luciferase reporter assay

The predicted miR-21-3p binding region in the sequence of the hsa_circRNA_101036 or TMTC 3′UTR was cloned and inserted into psiCHECK-2 vectors. Vectors containing a mutant binding region served as controls. The plasmids were constructed by Sangon Biotech (Shanghai, China) and co-transfected with miR-21-3p mimics/negative control mimics into OSCC cells. Luciferase activity at 48 h after transfection was quantified using a Dual-Luciferase Assay kit (TransGen, Beijing, China).

### 2.6. Transmission electron microscopy (TEM)

TEM was used to detect the morphology of endoplasmic reticulum in OSCC cells. Briefly, treated cells were fixed with 2.5 % glutaraldehyde, dehydrated with a graded ethanol series, embedded in Spurr resin, and cut into ultrathin sections. The sections were then stained with uranyl acetate and lead citrate and observed with a transmission electron microscope (JOEL, Japan).

### 2.7. Flow cytometry

Flow cytometry was used to detect apoptotic cells and reactive oxygen species (ROS). Treated OSCC cells were harvested and stained with Annexin V-FITC/propidium iodide (PI) (Apoptosis Detection Kit; Beyotime, Shanghai, China) to quantify the numbers of apoptotic cells. For ROS detection, OSCC cells were incubated with reagents in a ROS Assay Kit (Beyotime). The stained cells were subsequently used to detect positive signals with a flow cytometer (ThermoFisher Scientific) and determine the level of apoptosis or ROS.

### 2.8. Mouse xenograft model

All protocols for the mouse xenograft model were approved by Hainan General Hospital. BALB/c nude mice (male, 18–20 g body weight, 5–6 weeks old) were provided by the Experimental Animal Center of Sun Yat sen University (Guangzhou, China). The mice were randomly assigned to the following 4 groups (n = 5 per group): HSC3 cells transfected with Vector (HSC3-Vector); HSC3 cells transfected with hsa_circRNA_101036 overexpression plasmid (HSC3-Ov-circRNA); OECM-1 cells transfected with Vector (OECM-1-Vector); OECM-1 cells transfected with hsa_circRNA_101036 overexpression plasmid (OECM-1-Ov-circRNA). All plasmids were packaged in lentivirus and the cell lines were screened for stability after transfection. The corresponding cells were harvested and subcutaneously injected into the right dorsal region of BALB/c mice [24]. Subsequently, the mice were housed in cages in a room with a 12 h light/dark cycle at 22 °C ± 2 °C, and sufficient water and food was provided. Starting on day 10 after injection, the tumor volume ($V = \text{length} \times \text{width}^2 \times 0.5$) and body weight of each mouse was determined every 3 days. All animals were euthanized under excessive anesthesia on day 28. The tumors were harvested, weighed, and then stored in liquid nitrogen for further analysis. All animal experiments were approved by Hainan General Hospital (Med-Eth-Re [2022]44).

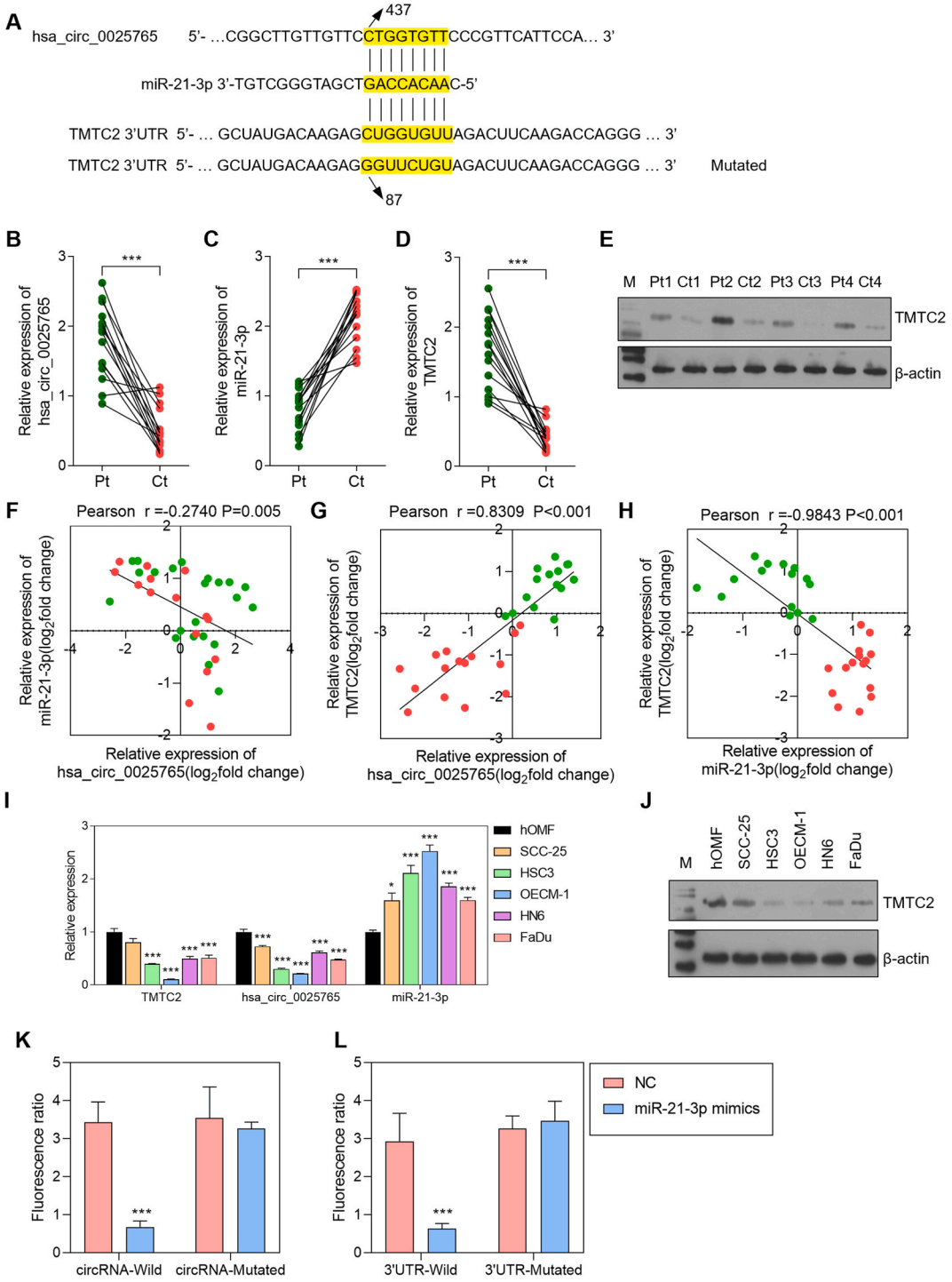


**Fig. 1. The correlations among hsa_circRNA_101036, miR-21-3p, and TMTC2 in OSCC.**

**A** The predicted binding site of miR-21-3p on hsa_circRNA_101036 and TMTC2. **B-D** The relative expression of hsa_circRNA_101036, miR-21-3p, and TMTC2 in tumor tissues (Ct) and paired para-carcinoma tissues (Pt) from oral squamous cell carcinoma (OSCC) patients as detected by quantitative PCR (qPCR). **E** The levels of TMTC2 protein in Ct and paired Pt from OSCC patients as detected by western blotting. **F–H** Correlations between the expression levels of hsa_circRNA_101036 and miR-21-3p, hsa_circRNA_101036 and TMTC2, and miR-21-3p and TMTC2 as analyzed by a Pearson analysis. **I** The relative levels of hsa_circRNA_101036, miR-21-3p, and TMTC2 expression in a human oral fibroblast cell line (hOMF) and 5 OSCC cell lines (SCC-25, HSC3, OECM-1, HN6, and FaDu). **J** The levels of TMTC2 protein in the human oral fibroblast cell line and OSCC cell lines. **K, L** Validation of the binding between hsa_circRNA_101036 and miR-21-3p, and miR-21-3p and TMTC2, as detected by the dual-luciferase reporter assay. $*p < 0.05$, $***p < 0.001$.

### 2.9. Statistical analysis

Quantitative data are presented as a mean value ± standard deviation (SD). All experiments were independently repeated three times. GraphPad Prism 8.0 software was used to perform statistical analyses according to the two-tailed unpaired Student's *t*-test and log-rank test. Pearson's correlation was used to analyze correlations between hsa_circRNA_101036 miR-21-3p expression and TMTC2 expression. A P-value <0.05 indicates a statistically significant difference.

## 3. Results

### 3.1. hsa_circRNA_101036 adsorbed miR-21-3p to stabilize TMTC2 mRNA

The database StarBase v.2.0, predicted an association between hsa_circRNA_101036 and miR-21-3p, and TargetScan 8.0, identified

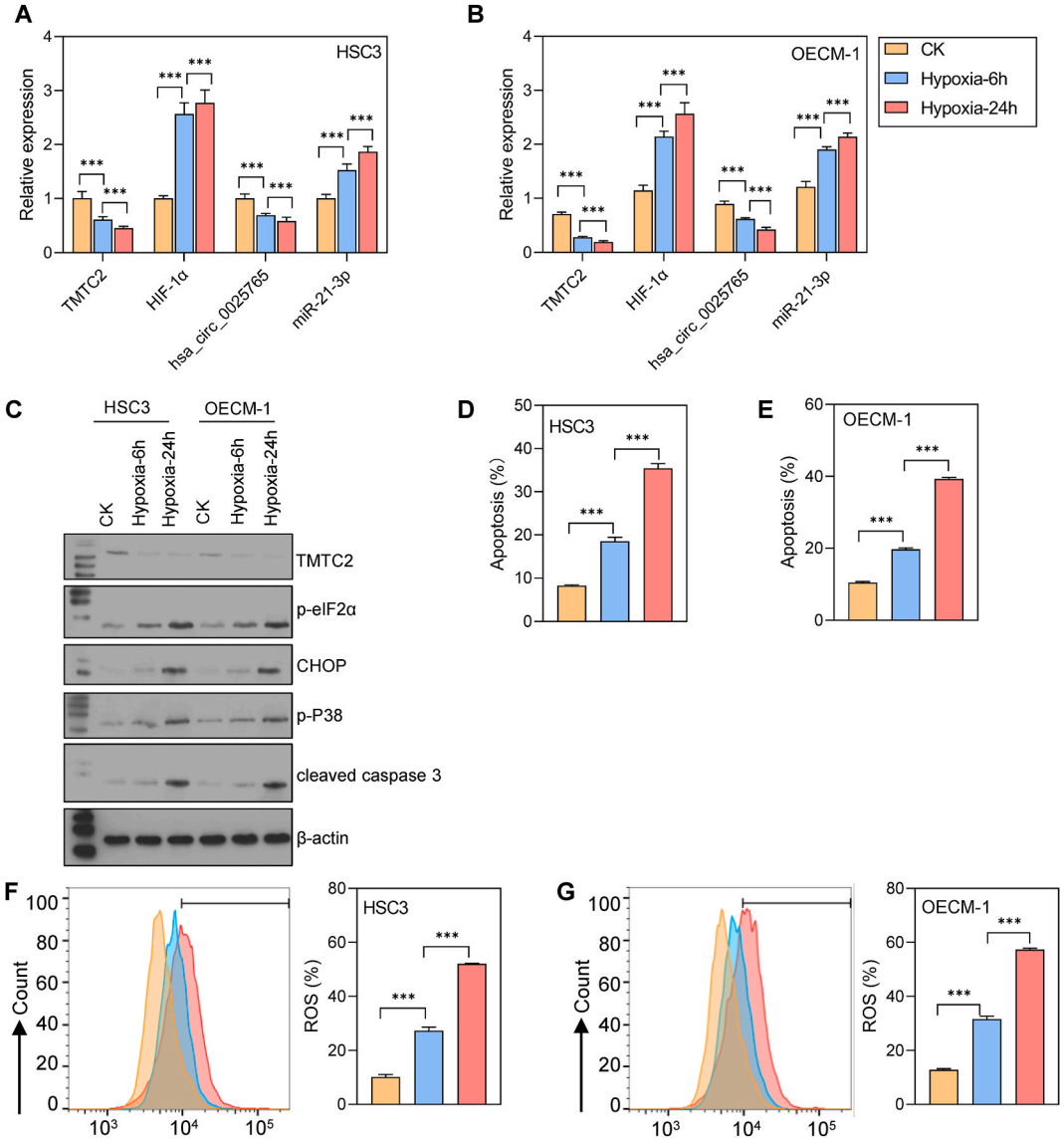


**Fig. 2.** The effects of hypoxia on endoplasmic reticulum (ER) stress, cell apoptosis, and ROS in HSC3 and OECM-1 cells.
**A, B** The relative expression of HIF-1α, hsa_circRNA_101036, miR-21-3p, and TMTC2 in HSC3 and OECM-1 cells with different duration of hypoxia treatment (0, 6, 24 h) as measured by qPCR. **C** The levels of TMTC2, phosphorylated (p-) eIF2α, CHOP, p-P38, and cleaved caspase 3 proteins in HSC3 and OECM-1 cells with hypoxia treatment as detected by western blotting. **D, E** The proportions of apoptotic HSC3 and OECM-1 cells with hypoxia treatment as quantified by flow cytometry. **F, G** The levels of ROS in HSC3 and OECM-1 cells with hypoxia treatment as quantified by flow cytometry. CK, cells with hypoxia treatment for 0 h ***$p < 0.001$.

3664 genes as potential targets of miR-21-3p. Among those target genes, we found that *e* was considered to be associated with ER stress. A bioinformatics analysis showed that both hsa_circRNA_101036 and TMTC2 have a potential binding site for miR-21-3p (Fig. 1A). QPCR was performed to analyze the correlations among hsa_circRNA_101036, miR-21-3p, and *TMTC2* expression in

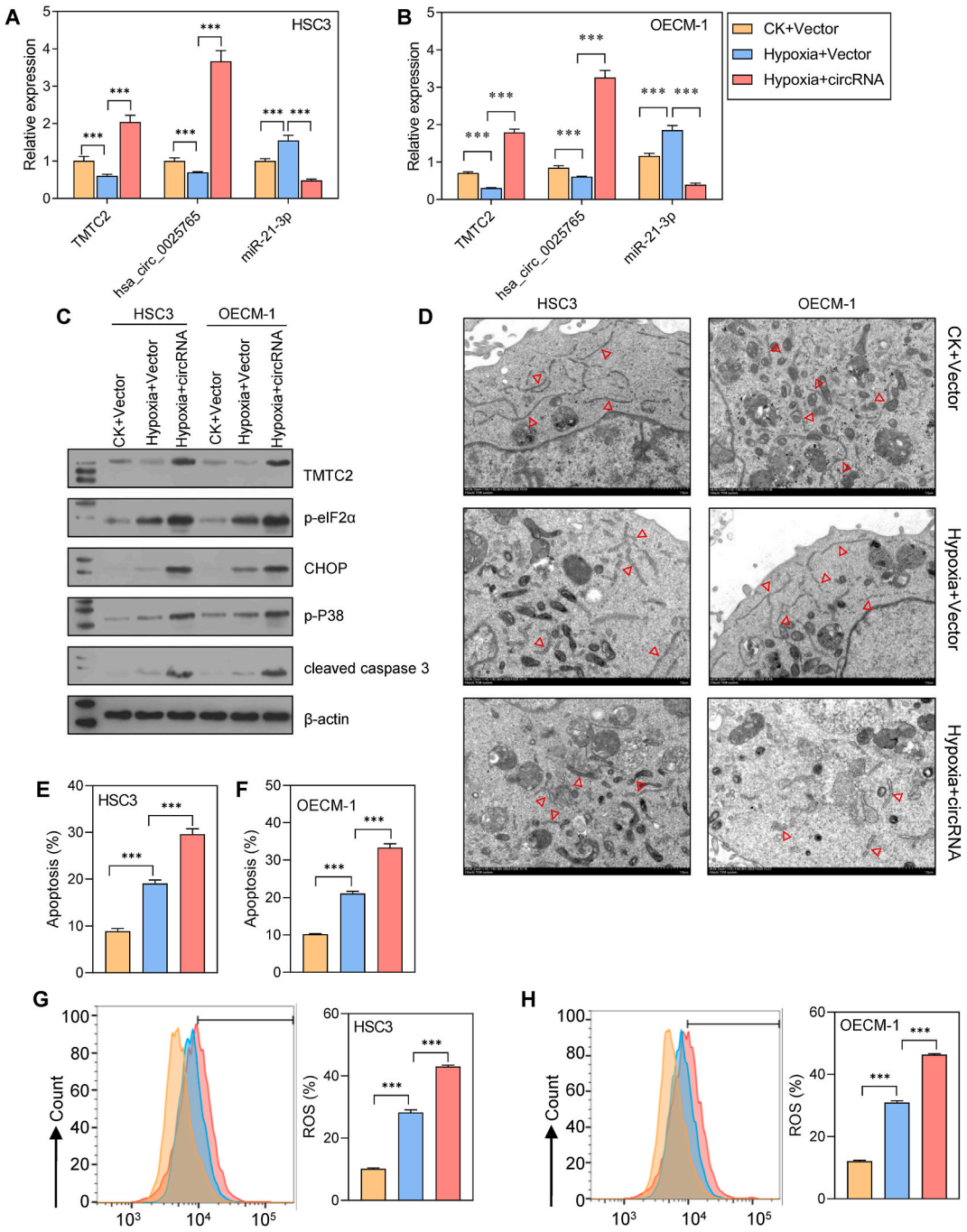


**Fig. 3.** The effects of hsa_circRNA_101036 overexpression on RS, cell apoptosis, and ROS on HSC3 and OECM-1 cells under conditions of hypoxia. **A, B** The relative levels of hsa_circRNA_101036, miR-21-3p, and TMTC2 expression in HSC3 and OECM-1 cells affected by hsa_circRNA_101036 overexpression. **C** The levels of TMTC2, *p*-eIF2α, CHOP, p-P38, and cleaved caspase 3 proteins in HSC3 and OECM-1 cells. **D** ER morphology as observed by transmission electron microscopy. The red triangle indicates endoplasmic reticulum. **E, F** hsa_circRNA_101036 overexpression increased the numbers of apoptotic HSC3 and OECM-1 cells. **G, H** hsa_circRNA_101036 overexpression increased the ROS levels in hypoxia-treated HSC3 and OECM-1 cells. CK + Vector, cells transfected with empty vector and cultured under normoxia. Hypoxia + Vector, cells transfected with empty vector and cultured under hypoxia. Hypoxia + circRNA, cells transfected with hsa_circRNA_101036 overexpression vector and cultured under hypoxia. ***$p < 0.001$.

OSCC tissues. The result showed that the levels of hsa_circRNA_101036 and TMTC2 expression were significantly decreased, while those of miR-21-3p were significantly elevated in tumor tissues when compared with para-carcinoma tissues (Fig. 1B–D). In addition, a Western blot analysis indicated that TMT2 expression was also downregulated at the protein level in OSCC tumor tissues (Fig. 1E). A Pearson's correlation analysis revealed that the levels of hsa_circRNA_101036 and TMTC2 were both negatively correlated with the level of miR-21-3p, and the level of hsa_circRNA_101036 was positively correlated with that of TMTC2 (Fig. 1F–H). We next compared the levels of hsa_circRNA_101036, miR-21-3p, and TMTC2 expression in 5 OSCC cell lines (SCC-25, HSC3, OECM-1, HN6, and FaDu) with those in a human oral fibroblast cell line (hOMF). Those results also revealed that the levels of hsa_circRNA_101036 and TMTC2 mRNA were lower in all 5 OSCC cell lines, while the levels of miR-21-3p were higher than those in the hOMF cells. Among the 5 OSCC cell lines, the levels of hsa_circRNA_101036, miR-21-3p, and TMTC2 in HSC3 and OECM-1 showed the greatest changes relative to hOMF (Fig. 1I). Therefore, HSC3 and OECM-1 cells were selected for further study. Moreover, TMTC2 expression at the protein level was also lower in all 5 OSCC cell lines than in hOMF cells (Fig. 1J). The results of dual-luciferase activity assays showed that the luciferase activity in cells co-transfected with wild-type hsa_circRNA_101036/TMTC2 and miR-21-3p mimics was markedly reduced when compared to the NC mimics group, while luciferase activity in the mutant group showed no significant change relative to the corresponding NC mimics group (Fig. 1K, L). Taken together, these findings suggest that hsa_circRNA_101036 functions as an miR-21-3p sponge that affects TMTC2 in OSCC cells.

### 3.2. *TMTC2 expression was inhibited and endoplasmic reticulum stress was induced under conditions of hypoxia*

To investigate the effect of a hypoxic environment on hsa_circRNA_101036, miR-21-3p, and TMTC2 mRNA expression in OSCC tumor tissue, HSC3 and OECM-1 cells were cultured under hypoxia to simulate the hypoxic condition *in vivo*. A qPCR analysis showed that the levels of hsa_circRNA_101036 and TMTC2 expression in both HSC3 and OECM-1 cells were significantly inhibited by hypoxia. Furthermore, the levels of hsa_circRNA_101036 were lower in cells with 24 h-hypoxia than in cells with 6 h-hypoxia. Meanwhile, the expression levels of HIF-1α and miR-21-3p showed the opposite trend (Fig. 2A and B). In addition, TMTC2 expression was decreased at the protein level under hypoxia (Fig. 2C). To evaluate the effects of ER stress and apoptosis on cells, the levels of *p*-eIF2α, CHOP, p-p38, and cleaved caspase 3 proteins were measured. Results showed that the levels of all those proteins were increased in a hypoxia duration-dependent manner in HSC3 and OECM-1 cells (Fig. 2C). Furthermore, flow cytometry analyses showed that the proportions of apoptotic cells and ROS-positive cells also increased according to hypoxia duration (Fig. 2D–G).

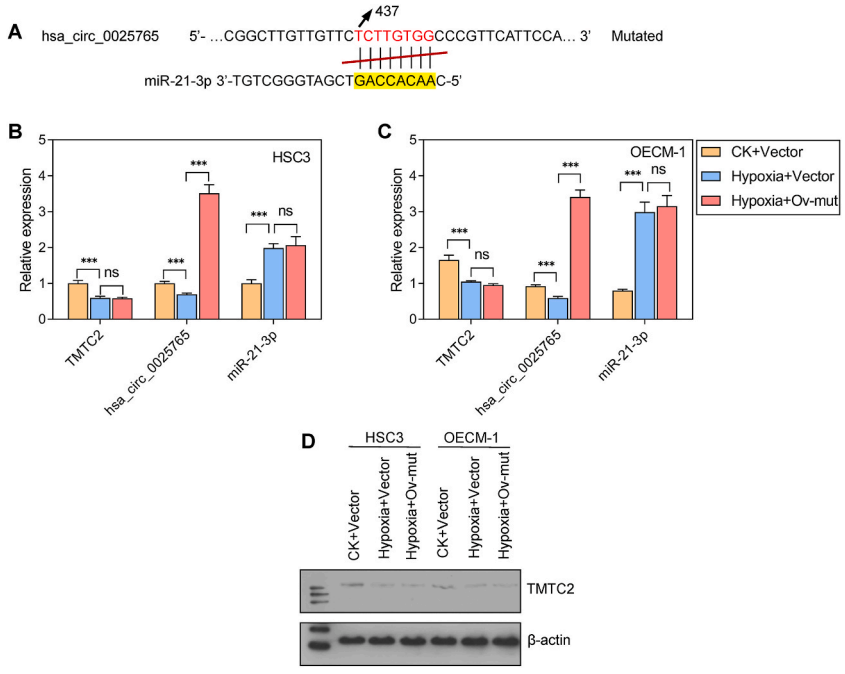


**Fig. 4.** Overexpression of mutant hsa_circRNA_101036 had no effect on the expression of hsa_circRNA_101036, miR-21-3p, and TMTC2 in HSC3 and OECM-1 cells.
**A** The sequence of mutant hsa_circRNA_101036. **B, C** The relative expression of hsa_circRNA_101036, miR-21-3p, and TMTC2 as detected by qPCR after overexpression of mutant hsa_circRNA_101036. **D** The levels of TMTC2 protein remained unchanged after overexpression of mutant hsa_circRNA_101036. CK + Vector, cells transfected with empty vector and cultured under normoxia. Hypoxia + Vector, cells transfected with empty vector and cultured under hypoxia. Hypoxia + Ov-mut, cells transfected with mutant hsa_circRNA_101036 overexpression vector and cultured under hypoxia. ns: not statistically significant; ***$p < 0.001$.

### 3.3. hsa_circRNA_101036 overexpression induced endoplasmic reticulum stress and apoptosis by up-regulating TMTC2 under hypoxia

To explore the function of hsa_circRNA_101036 in OSCC cells under hypoxia, hsa_circRNA_101036 was overexpressed in HSC3 and OECM-1 cells. hsa_circRNA_101036 overexpression was found to up-regulate TMTC2 and downregulate miR-21-3p in both HSC3 and OECM-1 cells (Fig. 3A and B). Furthermore, the levels of cleaved caspase 3, *p*-eIF2α, CHOP, and p-p38 were all increased by hsa_circRNA_101036 overexpression (Fig. 3C). Next, the intracellular ultrastructure of HSC3 and OECM-1 cells was examined by TEM. Those results showed that the endoplasmic reticulum was more shrunken in cells with hsa_circRNA_101036 overexpression under hypoxia (Fig. 3D). Meanwhile, the hsa_circRNA_101036 overexpression group had significantly higher proportions of apoptotic cells and levels of ROS (Fig. 3E–H). However, overexpression of mutant hsa_circRNA_101036 had no effect on miR-21-3p and TMTC2

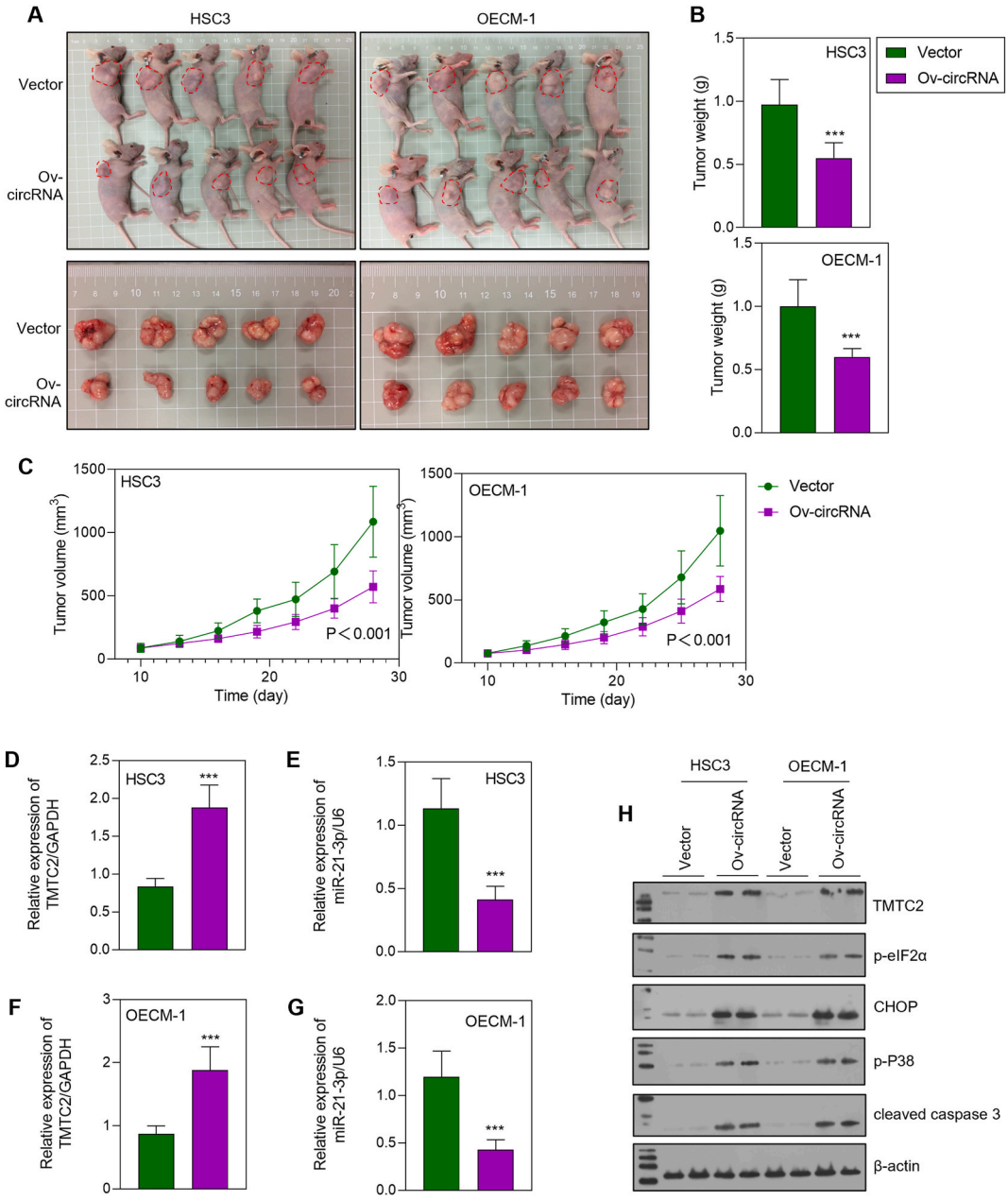


**Fig. 5.** The effect of hsa_circRNA_101036 overexpression on ER stress and tumorigenesis *in vivo*.
**A** Representative images of nude mice sacrificed on day 28 after injection and their corresponding tumor tissues. **B, C** Overexpression of hsa_circRNA_101036 significantly reduced tumor weight and tumor growth. **D-G** Relative expression of miR-21-3p and TMTC2 in tumor tissues as detected by qPCR. **H** The levels of TMTC2, *p*-eIF2α, CHOP, p-P38, and cleaved caspase 3 proteins in tumor tissues as detected by western blotting. Ov-circRNA: hsa_circRNA_101036 overexpression group; ***$p < 0.001$.

expression (Fig. 4A–D). Collectively, these findings suggest that hsa_circRNA_101036 functions as an miR-21-3p sponge to induce endoplasmic reticulum stress and ROS production, and promotes cell apoptosis by up-regulating TMTC2 under conditions of hypoxia.

### 3.4. hsa_circRNA_101036 had an anti-tumor function in vivo

To demonstrate the pro-apoptotic function of hsa_circRNA_101036 *in vivo*, HSC3 and OECM-1 cells overexpressing of hsa_circRNA_101036 (Ov-circRNA) or normal (Vector) HSC3 and OECM-1 cells were used in xenograft models. The tumor tissues on day 28 after injection are shown in Fig. 5A. The weights and volumes of tumors from the HSC3-Ov-circRNA and OECM-1-Ov-circRNA groups were significantly less than those from the HSC3-Vector and OECM-1-Vector groups, respectively (Fig. 5B and C). Next, the levels of miR-21-3p mRNA and TMTC2 mRNA in the tumor tissues were detected. The results showed that the levels of miR-21-3p mRNA were decreased, while those of TMTC2 mRNA were increased in tumors from the HSC3-Ov-circRNA and OECM-1-Ov-circRNA groups (Fig. 5D–G). Moreover, the levels of cleaved caspase 3, *p*-eIF2α, CHOP and p-p38 were all increased by overexpression of hsa_circRNA_101036 (Fig. 5H). Immunohistochemical results showed that caspase 3 was accumulated, and Ki67 levels were reduced in the overexpression group (Fig. 6A and B). These results indicated that hsa_circRNA_101036 could exert an anti-tumor function by up-

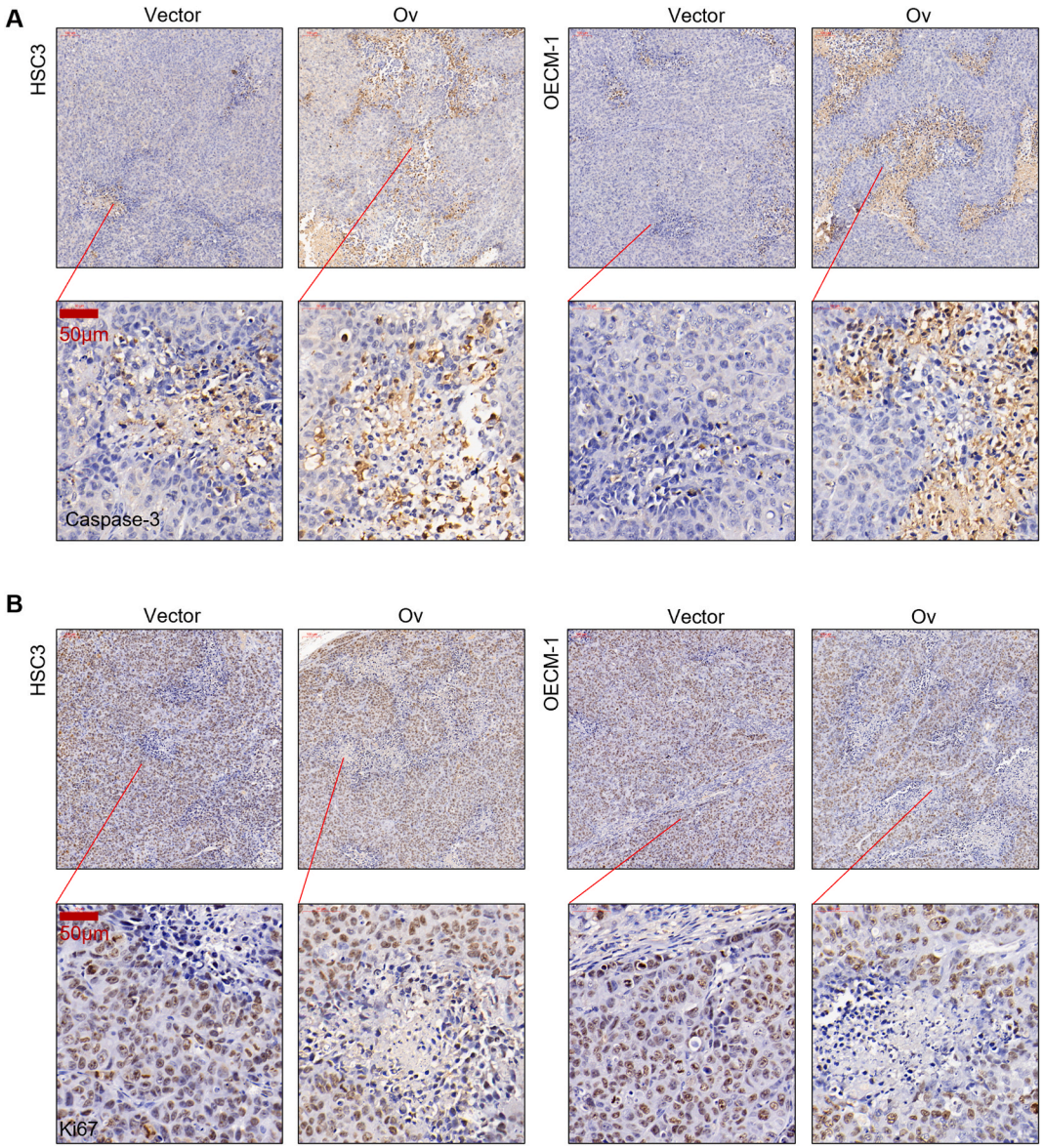


**Fig. 6.** hsa_circRNA_101036 overexpression regulated caspase 3 and Ki67 levels *in vivo*.
**A, B** The levels of caspase 3 and Ki67 proteins in tumor tissues were measured by an immunohistochemistry assay. The cells displayed in brown yellow color are positive for caspase 3 or Ki67 expression. Ov-circRNA: hsa_circRNA_101036 overexpression group; Scar bar: 50 μm.

regulating TMTC2 *in vivo*.

### 3.5. miR-21-3p interference provoked endoplasmic reticulum stress and apoptosis under hypoxia

To demonstrate the function of miR-21-3p, its inhibitor was transfected into HSC3 and OECM-1 cells. Under hypoxia, the levels of miR-21-3p were restrained by its inhibitor (Hypoxia + inhibitor vs. Hypoxia + NC groups) (Fig. 7A and B). Interestingly, the levels of TMTC2, *p*-eIF2α, CHOP, p-p38, and cleaved caspase 3 expression were all increased by the miR-21-3p inhibitor (Fig. 7C). Furthermore,

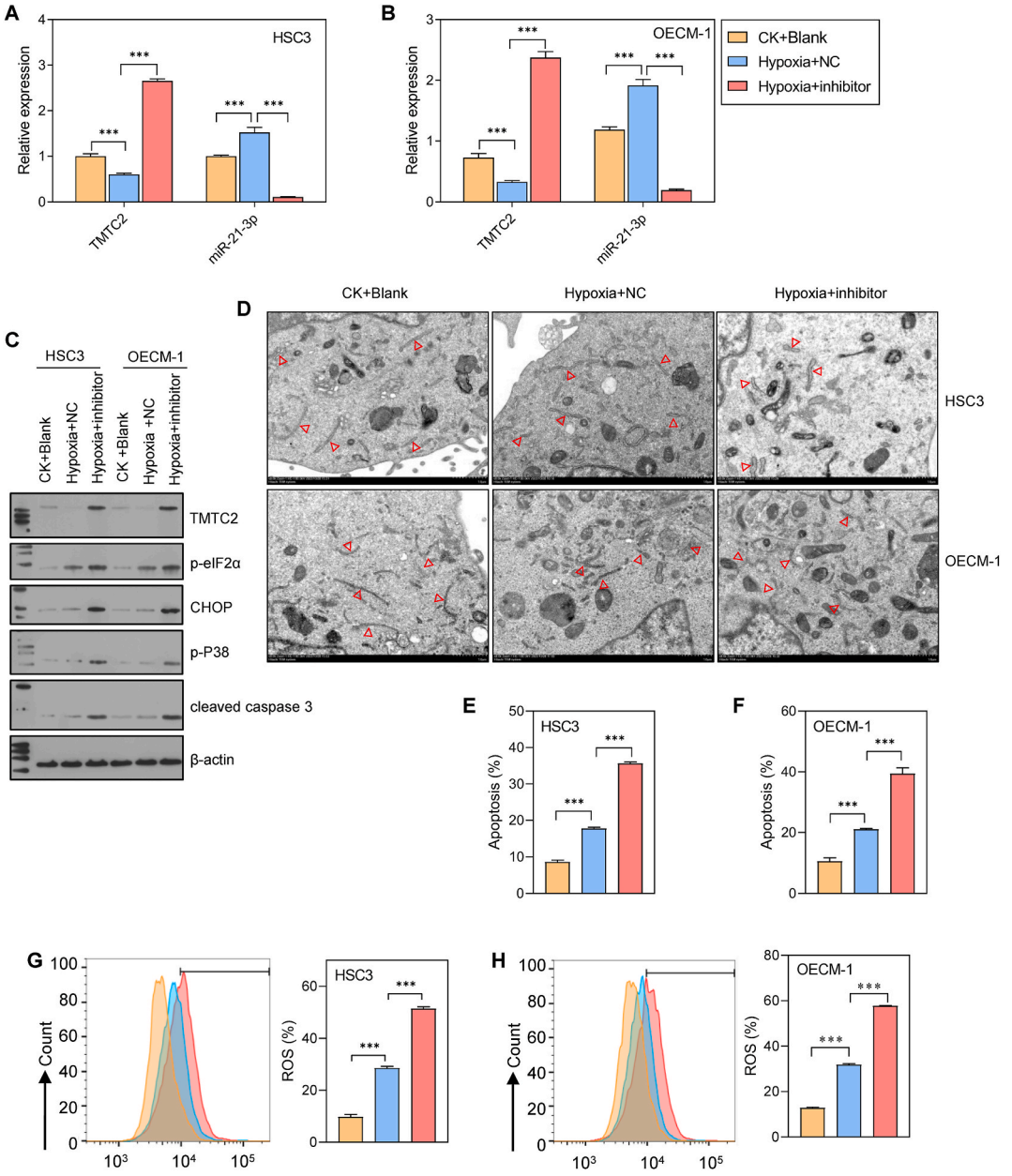


**Fig. 7. Interference by miR-21-3p promoted ER stress in HSC3 and OECM-1 cells under conditions of hypoxia.**
HSC3 and OECM-1 cells were transfected with the miR-21-3p inhibitor. **A, B** Relative levels of miR-21-3p and TMTC2 expression as detected by qPCR. **C** The levels of TMTC2, *p*-eIF2α, CHOP, p-P38, and cleaved caspase 3 proteins as detected by western blotting **D** The morphology of ER as observed under a transmission electron microscope. The red triangle indicates endoplasmic reticulum. **E-H** The miR-21-3p inhibitor increased the levels of apoptosis and ROS in hypoxia-treated HSC3 and OECM-1 cells. CK + Blank, cells cultured under normoxia with no transfection. Hypoxia + NC, cells transfected with the miRNA inhibitor negative control and cultured under hypoxia. Hypoxia + inhibitor, cells transfected with the miR-21-3p inhibitor and cultured under hypoxia. ***$p < 0.001$.

images obtained by TEM showed that the shape of the endoplasmic reticulum was shorter in the Hypoxia + inhibitor group than in the Hypoxia + NC group (Fig. 7D), and the levels of cell apoptosis and ROS were significantly higher in the Hypoxia + inhibitor group (Fig. 7E–H). These effects were consistent with those seen in cells overexpressing hsa_circRNA_101036, further indicating that hsa_circRNA_101036 regulates ER stress, ROS, and cell apoptosis in OSCC cells by sponging miR-21-3p under conditions of hypoxia.

## 4. Discussion

Non-coding RNA is transcribed by 75 % of the human genome, and those transcription products are involved in a wide range of biological regulatory functions. Numerous studies have found that non-coding RNA is dysregulated in tumors and participates in the progression of multiple tumors [25–27]. In this study, our results showed that hsa_circRNA_101036 was a sponge for miR-21-3p and promoted hypoxia-induced ER stress in OSCC.

Hypoxia is a characteristic of the microenvironment in solid tumors [28]. For normal cells, the damage caused by hypoxia is fatal. However, tumor cells can trigger the UPR to restore intracellular homeostasis and sustain their survival. Study has reported that hypoxia and chronic ER stress both induce chemoresistance [29]. Many factors and pathways have been found to regulate the UPR in tumor cells. Li et al. suggested that blocking TRPV4, a high-flux $Ca^{2+}$ channel, could alleviate ER stress mediated apoptosis in hypoxia-induced cardiomyocyte injury [30]. In pulmonary artery smooth muscle cells, hypoxia induces ER stress by promoting mitochondrial fragmentation [31]. In addition, Gao et al. found that circCDR1as was abnormally up-regulated in OSCC, and overexpression of circCDR1 as promoted ER stress by increasing the levels of eIF2α under hypoxia, and increasing cell viability [32]. In the present study, we also found that a circRNA, hsa_circRNA_101036, participated in regulating ER stress in OSCC. Hsa_circRNA_101036 expression was provoked in OSCC tissue and OSCC cells under conditions of hypoxia. Overexpression of hsa_circRNA_101036 could induce ER stress and up-regulate the levels of UPR-related proteins, including eIF2α and CHOP, both *in vitro* and *in vivo*. Regulation of ER stress by circRNA under hypoxic conditions was also found to occur in periodontal ligament stem cells during osteogenic differentiation. Indeed, the roles played by circRNAs in ER homeostasis need further exploration.

MiRNAs are another vital factor that can directly or indirectly regulate the three UPR pathways. For the ATF6-mediated pathway, miRNAs such as miR-103, miR-107 [33], miR-149 [34], and miR-221 [35], can directly or indirectly target ATF6α to regulate its expression and activity. For the IRE1α-mediated pathway, miR-1291 directly targets the 5′-UTR of IRE1α [36]. It also been reported that miRNAs regulate the PERK-regulated pathway, which is chiefly modulated by eIF2α and CHOP [37]. Furthermore, another study reported that miR-30b-5p and miR-30 cc-5p targeted eIF2α, and activation of CHOP was an important pathway for inducing ER stress-related apoptosis [25]. In addition, miR-146a was found to reduce the levels of CHOP mRNA and induce cisplatin resistance in lung cancer [38]. MiR-657 overexpression can offset the up-regulation of CHOP, *p*-ATF2, and PARP cleavage expression and inhibit the cell apoptosis caused by *Spatholobus suberectus* Dunn (SSD) [39]. Some miRNAs are related to the expression of multiple components in the UPR pathway. In colorectal cancer, miR-451a can induce ER stress by targeting the 5′-UTR of BAP31. MiR-451a overexpression or BAP31 interference can upregulate the levels of PERK, eIF2α, ATF4, and CHOP proteins, and thereby inhibit tumor cell proliferation [40]. In this study, we speculated that an miR-21-3p inhibitor could aggravate ER stress and increase the levels of *p*-eIF2α and CHOP, indicating that miR-21-3p functions as an oncogene in OSCC.

ER stress can affect miRNA expression. Jiang et al. discovered that miR-1281 could be regulated by ER stress via direct binding of p53 to the miR-1281 promoter [41]. Wang et al. found that an ER stress inducer could significantly downregulate the levels of 3 miRNAs in HCC cells [42]. However, few studies have reported the effect of ER stress on circRNA.

MiR-21-3p has high specificity and sensitivity for predicting cervical lymph node metastasis in OSCC patients [43]. Increased levels of miR-21-3p in OSCC tissues have also been found in Chinese hamsters [44]. In addition, study has found that miR-21-3p stimulates OSCC cell invasion [45]. In other cancers, miR-21-3p plays important roles in drug resistance [46], cell growth [47], and T cell exhaustion [48]. Consistent with those studies, we found that miR-21-3p was markedly up-regulated in OSCC tissues when compared to corresponding para-carcinoma tissues. Our results also showed that an miR-21-3p inhibitor could promote cell apoptosis and ROS production by aggravating ER stress.

CircRNAs and miRNAs are not only related to ER stress, but also involved in tumorigenesis, proliferation, metastasis, and the efficacy of cancer therapy, either as oncogenes or tumor suppressors, via various mechanisms. In addition, they are aberrantly expressed in tumor tissues and resistant to exonucleases and RNase R. Due to these properties, circRNAs and miRNAs are potential markers for use in the diagnosis and prognosis of cancers, as well as promising targets for cancer therapy. For example, circFGFR1 was found to be a sponge of miR-381–3p and accelerate NSCLC progression and anti-PD-1 resistance, and therefore be a possible target for treating NSCLC [49]. Circ_0001874 and Circ_0001971 in salivary glands were found to be biomarkers for diagnosing OSCC [50]. We found that hsa_circRNA_101036 and miR-21-3p were regulators of the UPR pathway, which has a pro-oncogenic function in cancer development and is unfavorable for cancer therapy. Therefore, hsa_circRNA_101036 and miR-21-3p may be promising signatures for the diagnosis of cancer, as well as targets for drug treatment of cancer.

The TMTC family in humans includes four genes, all of which code for proteins that have a C-terminal with transmembrane regions and intermittent loops, and a C-terminal with 10 tetratricopeptide repeats (TPR) that support protein-protein interactions. They orient in the ER and TPR domains of the ER lumen [51]. TMTC1 and TMTC2 were reported to be adapter proteins that influence calcium homeostasis in ER [52]. Overexpression of TMTC2 causes a reduction of calcium released from the ER following stimulation, whereas knockdown of TMTC2 increases the amount of calcium released. TMTC3 may play a role in the ER stress response [53]. TMTC4 is associated with the UPR [54]. Collectively, the TMTC family is commonly associated with ER stress. In the present study, our results showed that *TMTC2* was a target of miR-21-3p. In HSC3 and OECM-1 cells, miR-21-3p knockdown promoted TMTC2 expression under hypoxic conditions. Meanwhile, *p*-eIF2α and CHOP, two proteins in the UPR pathway, were also up-regulated. We found that the

morphology of ER became wrinkled and shorter, indicating an exacerbated level of ER stress. Therefore, a high level of TMTC2 expression suggests severe ER stress, and miR-21-3p might maintain ER homeostasis by targeting TMTC2. However, the functional mechanism of TMTC2 in ER stress occurring OSCC remains unknown, which is a limitation of this study. Taken together, hsa_circRNA_101036 was found to induce ER stress by sponging miR-21-3p to stabilize TMTC2 mRNA. It is important to note that OSCC is a complex disease that has multiple molecular pathways and factors involved in its pathogenesis. Other pathways and factors may also contribute to the development and progression of OSCC, and their impact on our current findings should be considered in future studies.

## 5. Conclusion

In conclusion, hsa_circRNA_101036 was found to be a negative regulator of miR-21-3p that competes with TMTC2 to bind with miR-21-3p, which increases TMTC2 expression, ER stress, cell apoptosis, and ROS production. Hsa_circRNA_101036 and miR-21-3p might be biomarkers for OSCC, and targets for OSCC treatment.

## Data availability statement

All data was included in in article.

## Ethics statement

All procedures performed in studies involving human participants were in accordance with the ethical standards of the Medical Ethics Committee of Hainan General Hospital (Med-Eth-Re[2023]44) and with the 1964 Helsinki Declaration and its later amendments or comparable ethical standards. All animal experiments were carried out strictly in accordance with international ethical guidelines and the National Institutes of Health Guide concerning the Care and Use of Laboratory Animals. All animal experiments were approved by Hainan General Hospital (Med-Eth-Re [2022]44).

## CRediT authorship contribution statement

**Wei Deng:** Writing – review & editing, Resources, Project administration, Conceptualization. **Juan Fu:** Methodology, Formal analysis, Data curation. **Shigeng Lin:** Investigation, Formal analysis, Data curation. **Qitao Wen:** Visualization, Validation, Supervision, Software, Methodology. **Liangbin Fu:** Writing – original draft, Visualization. **Xiaoze Chen:** Visualization, Validation, Supervision, Software, Methodology.

## Declaration of competing interest

The authors declare the following financial interests/personal relationships which may be considered as potential competing interestsWei Deng reports financial support was provided by Hainan General Hospital (Hainan Affiliated Hospital of Hainan Medical University).

## Acknowledgement

This study was supported by Hainan Provincial Natural Science Foundation of China (No. 821RC681 and No. 820MS136).

## Appendix A. Supplementary data

Supplementary data to this article can be found online at https://doi.org/10.1016/j.heliyon.2024.e32969.

## References

[1] W.M. Mendenhall, A.L. Holtzman, R. Dagan, et al., Current role of radiotherapy in the management of oral cavity squamous cell carcinoma, Craniomaxillofac Trauma Reconstr 14 (1) (2021) 79–83.
[2] J.M. Qian, J.D. Schoenfeld, Radiotherapy and immunotherapy for head and neck cancer: current evidence and challenges, Front. Oncol. 10 (2020) 608772.
[3] J. Li, J. Yang, P. Zhou, et al., Circular RNAs in cancer: novel insights into origins, properties, functions and implications, Am. J. Cancer Res. 5 (2) (2015) 472–480.
[4] Y. Chen, C. Li, C. Tan, et al., Circular RNAs: a new frontier in the study of human diseases, J. Med. Genet. 53 (6) (2016) 359–365.
[5] W.R. Jeck, J.A. Sorrentino, K. Wang, et al., Circular RNAs are abundant, conserved, and associated with ALU repeats, Rna 19 (2) (2013) 141–157.
[6] L. Chen, G. Shan, CircRNA in cancer: fundamental mechanism and clinical potential, Cancer Lett. 505 (2021) 49–57.
[7] Y. Gao, J. Wang, Y. Zheng, et al., Comprehensive identification of internal structure and alternative splicing events in circular RNAs, Nat. Commun. 7 (2016) 12060.
[8] X. Guo, C. Gao, D.H. Yang, et al., Exosomal circular RNAs: a chief culprit in cancer chemotherapy resistance, Drug Resist. Updates 67 (2023) 100937.

[9] J. Tan, B. Yang, H. Zhong, et al., Circular RNA circEMB promotes osteosarcoma progression and metastasis by sponging miR-3184-5p and regulating EGFR expression, Biomark Research 11 (1) (2023) 3.
[10] H. Chen, X. Wang, H. Cheng, et al., CircRNA circRREB1 promotes tumorigenesis and progression of breast cancer by activating Erk1/2 signaling through interacting with GNB4, Heliyon 10 (7) (2024) e28785.
[11] V.M. Conn, M. Gabryelska, J. Toubia, et al., Circular RNAs drive oncogenic chromosomal translocations within the MLL recombinome in leukemia, Cancer Cell 41 (6) (2023) 1309–1326.
[12] H. Zhang, Z. Wang, Z. Zhang, Hsa_circ_0009128 mediates progression of oral squamous cell carcinoma by influencing MMP9, Oral Dis 29 (2021) 661–667.
[13] W. Su, Y. Wang, F. Wang, et al., Hsa_circ_0005379 regulates malignant behavior of oral squamous cell carcinoma through the EGFR pathway, BMC Cancer 19 (1) (2019) 400.
[14] D. Shi, H. Li, J. Zhang, et al., CircGDI2 regulates the proliferation, migration, invasion and apoptosis of OSCC via miR-454-3p/FOXF2 Axis, Cancer Manag. Res. 13 (2021) 1371–1382.
[15] W. Deng, J. Fu, T. Wang, et al., Hsa_circRNA_101036 acts as tumor-suppressor in oral squamous cell carcinoma cells via inducing endoplasmic reticulum stress, Eur. Rev. Med. Pharmacol. Sci. 24 (11) (2020) 6111–6121.
[16] P.O. DE Lima, C. Jorge, D. Oliveira, et al., Hypoxic condition and prognosis in oral squamous cell carcinoma, Anticancer Res. 34 (2) (2014) 605–612.
[17] M. Koritzinsky, F. Levitin, T. van den Beucken, et al., Two phases of disulfide bond formation have differing requirements for oxygen, J. Cell Biol. 203 (4) (2013) 615–627.
[18] N. Sheshadri, D.K. Poria, S. Sharan, et al., PERK signaling through C/EBPδ contributes to ER stress-induced expression of immunomodulatory and tumor promoting chemokines by cancer cells, Cell Death Dis. 12 (11) (2021) 1038.
[19] M. Akman, D.C. Belisario, I.C. Salaroglio, et al., Hypoxia, endoplasmic reticulum stress and chemoresistance: dangerous liaisons, J. Exp. Clin. Cancer Res. 40 (1) (2021) 28.
[20] M. Śniegocka, F. Liccardo, F. Fazi, et al., Understanding ER homeostasis and the UPR to enhance treatment efficacy of acute myeloid leukemia, Drug Resist. Updates 64 (2022) 100853.
[21] E. Delbrel, A. Soumare, A. Naguez, et al., HIF-1α triggers ER stress and CHOP-mediated apoptosis in alveolar epithelial cells, a key event in pulmonary fibrosis, Sci. Rep. 8 (1) (2018) 17939.
[22] H.M. Ali, A. Maksimenko, G. Urbinati, et al., Effects of silencing the RET/PTC1 oncogene in papillary thyroid carcinoma by siRNA-squalene nanoparticles with and without fusogenic companion GALA-cholesterol, Thyroid 24 (2) (2014) 327–338.
[23] G. Urbinati, H.M. Ali, Q. Rousseau, et al., Antineoplastic effects of siRNA against TMPRSS2-ERG junction oncogene in prostate cancer, PLoS One 10 (5) (2015) e0125277.
[24] G. Urbinati, I. de Waziers, M. Slamiç, et al., Knocking down TMPRSS2-ERG fusion oncogene by siRNA could be an alternative treatment to flutamide, Mol. Ther. Nucleic Acids 5 (3) (2016) e301.
[25] T. Zhao, J. Du, H. Zeng, Interplay between endoplasmic reticulum stress and non-coding RNAs in cancer, J. Hematol. Oncol. 13 (1) (2020) 163.
[26] M. Śniegocka, F. Liccardo, F. Fazi, et al., Understanding ER homeostasis and the UPR to enhance treatment efficacy of acute myeloid leukemia, J. Nanobiotechnol. 21 (1) (2023) 45.
[27] M. Śniegocka, F. Liccardo, F. Fazi, et al., Understanding ER homeostasis and the UPR to enhance treatment efficacy of acute myeloid leukemia, Chem. Biol. Interact. 347 (2023) 110412.
[28] X. Zhao, F.K. Amevor, X. Xue, et al., Remodeling the hepatic fibrotic microenvironment with emerging nanotherapeutics: a comprehensive review, J. Nanobiotechnol. 21 (1) (2023) 121.
[29] M. Akman, D.C. Belisario, I.C. Salaroglio, et al., Hypoxia, endoplasmic reticulum stress and chemoresistance: dangerous liaisons, J. Exp. Clin. Cancer Res. 40 (1) (2021) 28.
[30] X. Li, K. Lu, S. Guo, et al., TRPV4 blockade alleviates endoplasmic reticulum stress mediated apoptosis in hypoxia-induced cardiomyocyte injury, Cell Signnaling 114 (2024) 110973.
[31] B. Zhuan, X. Wang, M.D. Wang, et al., Hypoxia induces pulmonary artery smooth muscle dysfunction through mitochondrial fragmentation-mediated endoplasmic reticulum stress, Aging (Albany NY) 12 (23) (2020) 23684–23697.
[32] L. Gao, Z.C. Dou, W.H. Ren, et al., CircCDR1as upregulates autophagy under hypoxia to promote tumor cell survival via AKT/ERK(½)/mTOR signaling pathways in oral squamous cell carcinomas, Cell Death Dis. 10 (10) (2019) 745.
[33] Z. Zhang, S. Wu, S. Muhammad, et al., miR-103/107 promote ER stress-mediated apoptosis via targeting the Wnt3a/β-catenin/ATF6 pathway in preadipocytes, J. Lipid Res. 59 (5) (2018) 843–853.
[34] Z. Chen, Y. Liu, L. Yang, et al., MiR-149 attenuates endoplasmic reticulum stress-induced inflammation and apoptosis in nonalcoholic fatty liver disease by negatively targeting ATF6 pathway, Immunol. Lett. 222 (2020) 40–48.
[35] I.K. Oglesby, R. Agrawal, M.A. Mall, et al., miRNA-221 is elevated in cystic fibrosis airway epithelial cells and regulates expression of ATF6, Mol Cell Pediatr 2 (1) (2015) 1.
[36] M. Maurel, N. Dejeans, S. Taouji, et al., MicroRNA-1291-mediated silencing of IRE1α enhances Glypican-3 expression, Rna 19 (6) (2013) 778–788.
[37] T. Kim, C.M. Croce, MicroRNA and ER stress in cancer, Semin. Cancer Biol. 75 (2021) 3–14.
[38] W. Tan, Y. Liao, Y. Qiu, et al., miRNA 146a promotes chemotherapy resistance in lung cancer cells by targeting DNA damage inducible transcript 3 (CHOP), Cancer Lett. 428 (2018) 55–68.
[39] H.J. Lim, M.N. Park, C. Kim, et al., MiR-657/ATF2 signaling pathway has a critical role in Spatholobus suberectus Dunn extract-induced apoptosis in U266 and U937 cells, Cancers 11 (2) (2019).
[40] K. Xu, B. Han, Y. Bai, et al., MiR-451a suppressing BAP31 can inhibit proliferation and increase apoptosis through inducing ER stress in colorectal cancer, Cell Death Dis. 10 (3) (2019) 152.
[41] J. Jiang, B. Ma, X. Li, et al., MiR-1281, a p53-responsive microRNA, impairs the survival of human osteosarcoma cells upon ER stress via targeting USP39, Am. J. Cancer Res. 8 (9) (2018) 1764–1774.
[42] Q. Duan, X. Wang, W. Gong, et al., ER stress negatively modulates the expression of the miR-199a/214 cluster to regulates tumor survival and progression in human hepatocellular cancer, PLoS One 7 (2) (2012) e31518.
[43] K.B. Jadhav, V. Shah, N. Chauhan, et al., Expression of microRNA-21 in saliva and tumor tissue of patients with oral squamous cell carcinoma: a predictor of cervical lymph node metastasis, Oral Surg Oral Med Oral Pathol Oral Radiol 133 (1) (2022) 60–69.
[44] G.Q. Xu, L.H. Li, J.N. Wei, et al., Identification and profiling of microRNAs expressed in oral buccal mucosa squamous cell carcinoma of Chinese hamster, Sci. Rep. 9 (1) (2019) 15616.
[45] H.H. Tseng, Y.K. Tseng, J.J. You, et al., Next-generation sequencing for microRNA profiling: MicroRNA-21-3p promotes oral cancer metastasis, Anticancer Res. 37 (3) (2017) 1059–1066.
[46] R.C. Pink, P. Samuel, D. Massa, et al., The passenger strand, miR-21-3p, plays a role in mediating cisplatin resistance in ovarian cancer cells, Gynecol. Oncol. 137 (1) (2015) 143–151.
[47] T.F. Lo, W.C. Tsai, S.T. Chen, MicroRNA-21-3p, a berberine-induced miRNA, directly down-regulates human methionine adenosyltransferases 2A and 2B and inhibits hepatoma cell growth, PLoS One 8 (9) (2013) e75628.
[48] Z. Han, R.J. Estephan, X. Wu, et al., MicroRNA regulation of T-cell exhaustion in cutaneous T cell lymphoma, J. Invest. Dermatol. 142 (3 Pt A) (2022) 603–612. e607.
[49] P.F. Zhang, X. Pei, K.S. Li, et al., Circular RNA circFGFR1 promotes progression and anti-PD-1 resistance by sponging miR-381-3p in non-small cell lung cancer cells, Mol. Cancer 18 (1) (2019) 179.
[50] S.Y. Zhao, J. Wang, S.B. Ouyang, et al., Salivary circular RNAs Hsa_Circ_0001874 and Hsa_Circ_0001971 as novel biomarkers for the diagnosis of oral squamous cell carcinoma, Cell. Physiol. Biochem. 47 (6) (2018) 2511–2521.

[51] B. Eisenhaber, S. Sinha, C.K. Jadalanki, et al., Conserved sequence motifs in human TMTC1, TMTC2, TMTC3, and TMTC4, new O-mannosyltransferases from the GT-C/PMT clan, are rationalized as ligand binding sites, Biol. Direct 16 (1) (2021) 4.
[52] J.C. Sunryd, B. Cheon, J.B. Graham, et al., TMTC1 and TMTC2 are novel endoplasmic reticulum tetratricopeptide repeat-containing adapter proteins involved in calcium homeostasis, J. Biol. Chem. 289 (23) (2014) 16085–16099.
[53] M. Racapé, J.P. Duong Van Huyen, R. Danger, et al., The involvement of SMILE/TMTC3 in endoplasmic reticulum stress response, PLoS One 6 (5) (2011) e19321.
[54] J. Li, O. Akil, S.L. Rouse, et al., Deletion of Tmtc4 activates the unfolded protein response and causes postnatal hearing loss, J. Clin. Invest. 128 (11) (2018) 5150–5162.